ELSEVIER

Catalysis Today 76 (2002) 221–233

CATALYSIS TODAY

www.elsevier.com/locate/cattod

Photocatalytic degradation of short-chain organic diacids

Maria Isabel Franch, José Antonio Ayllón, José Peral, Xavier Domènech*

Departament de Química, Universitat Autònoma de Barcelona, 08193 Bellaterra (Barcelona), Spain

Abstract

The heterogeneous photocatalytic oxidation of fumaric, maleic and oxalic acids over TiO_2 has been investigated. For aqueous suspensions at pH lower than the point of zero charge (pzc) of TiO_2, the photocatalytic degradation of the three studied diacids follows the Langmuir–Hinshelwood kinetic model, with the rate constant of the process decreasing in the order oxalic acid $>$ maleic acid $\cong$ fumaric acid. At these low pH media, the adsorption of the organic diacids onto TiO_2 particles is a key feature for their degradation, which is initiated by a photo-Kolbe process. For fumaric and maleic acids, a *cis–trans* isomerisation induced by the interaction between adsorbed molecule and semiconductor surface occurs. At pH's higher than the pzc of TiO_2 the rate of oxalic acid oxidation decreases noticeably, while fumaric and maleic acids are both efficiently degraded in homogeneous phase by reacting with $OH^{\bullet}$ radicals photochemically generated on the TiO_2 surface, giving rise to a significant increment of both isomers degradation rate with increasing pH. At these pH's higher than the pzc of the TiO_2, the three studied diacids show a very low degree of adsorption onto the semiconductor surface and no evidence of *cis–trans* isomerisation for both maleic and fumaric acids is detected. In accordance with the observed pH effects on degradation rate and over detected intermediates, a different mineralisation pathway is proposed as function of initial pH.

Keywords: Photocatalytic degradation; Short-chain organic diacids; *cis–trans* Isomerisation

1. Introduction

In the last years, heterogeneous semiconductor photocatalysis has been one of the most studied advanced oxidation processes (AOPs) for degradation of organic contaminants in aqueous phase, due to the mild conditions used to generate $OH^{\bullet}$ radicals and to the high capability to eliminate biorecalcitrant contaminants [1–3]. The photocatalytically mediated mineralisation of aromatic compounds has been the subject of numerous investigations [2,3]. For these organic contaminants, it has been observed that, in general, the time period required to achieve the dearomatisation of the contaminant species is clearly lower than the time needed to eliminate the products resulting from the aromatic ring breaking [1]. The aliphatic intermediates most frequently encountered during the degradation of aromatic compounds are short-chain carboxylic diacids, as maleic, fumaric and oxalic acids, which have been detected during the mineralisation of a variety of organic chemicals [4–10]. Then, the understanding of the kinetics and mechanism of degradation of these compounds can assist us for the ascertaining of the better conditions to perform the mineralisation of recalcitrant organic compounds.

Among the short-chain organic diacids, oxalic acid photocatalytic degradation has been the most investigated, because of its role as sacrificial agent to decrease electron–hole recombination and increase the efficiency of some photoreduction process at the

* Corresponding author.
E-mail address: xavier.domenech@uab.es (X. Domènech).

0920-5861/02/$ – see front matter
PII: S0920-5861(02)00221-3

semiconductor–electrolyte interphase [11–15]. The objective of this work is to investigate the photocatalytic degradation of maleic, fumaric and oxalic acids, and also the corresponding mixtures in multicompound systems, using TiO_2 as semiconductor catalyst, with the aim to study the kinetics and the mechanism of photodegradation and to find the better experimental conditions to carry out this process.

2. Experimental

2.1. Reagents

All chemicals mentioned hereafter were, at least, of reagent grade and used as received. Solutions were prepared with water purified in a Millipore Milli-Q system. TiO_2 Degussa P25 (80% anatase–20% rutile, 59.1 m^2/g, non-porous) was used as photocatalyst.

2.2. Photocatalytic and adsorption studies

Photocatalytic and adsorption experiments were performed in a cylindrical Pyrex reactor provided with a thermostatic jacket. All the experiments were performed at $25 \pm 0.1\,^{\circ}C$. Aqueous suspensions were magnetically stirred and for all experiments air was continuously bubbled through the solution. $HClO_4$ and NaOH (aq) were used to adjust the initial pH values. Substrate aqueous solution (0.4 l) at various initial concentrations and TiO_2 powder (0.600 g) were introduced in the reactor and kept in the dark until adsorption equilibrium was reached. In photocatalytic degradation experiments, after a dark equilibration is attained, irradiation of solutions were carried out using a medium pressure mercury vapour lamp Philips HPK 125 W. The light source was placed in a water-cooled Pyrex jacket that filtered UV ($\lambda < 290$) nm and IR radiations. The incident radiant flux measured by using an uranil actinometer was 8.31×10^{-6} einstein l^{-1} s^{-1}.

2.3. Analytical methods

UV-vis spectra were registered with an HP-8453 diode array spectrometer. The concentration of the studied diacids and detected intermediates during photodegradation process was measured by HPLC analysis. The HPLC system was constituted by an LC-10 AT VP pump (Shimadzu), a UV-vis absorbance detector (Applied Absorbance Biosystems 759A) adjusted at 210 nm, and an HP 3394A integrator. The stationary phase was an Aminex-87-H column (300×7.8 mm^2). The mobile phase employed was a 0.005 mol l^{-1} H_2SO_4 aqueous solution at isocratic flow rate of 0.75 ml/min. Total organic carbon (TOC) determination was carried out with a TOC-5000 SHIMADZU Total Carbon Analyser provided with a NDIR detector. Before analysis, samples were filtered trough 0.45 μm pore size nylon filter in order to remove any particulates.

3. Results and discussion

The TiO_2 photocatalytic degradation in aqueous solutions of maleic, fumaric and oxalic acids, and the corresponding mixtures in multicompound systems, have been studied. Prior to carry out the kinetic study of the maleic, fumaric and oxalic acid photocatalytic oxidation, some blank experiments were performed at 1×10^{-3} mol l^{-1} diacid aqueous solutions at initial pH = 3. Thus, in the dark and in the absence of TiO_2, after the suspensions were air bubbled during 1 h, no reduction of initial organic concentration was observed. At the same experimental conditions but under UV-illumination, only a 2% of maleic and fumaric acid elimination has been detected, while for oxalic acid a decrease of about 8% of the initial concentration after 1 h of irradiation occurs. It must be pointed out that UV-vis absorption spectra, for $\lambda > 290$ nm, of each of the studied diacids do not show any variation within the pH range comprised between 3 and 9, consequently the obtained results about photochemical degradation applies to all this pH range. Finally, in the dark but in presence of TiO_2, a certain degree of adsorption of the organic compound is observed; after 5 min of stirring a limiting value of adsorbed organic is attained: 8% for both maleic and fumaric acids, and 13% for oxalic acid.

3.1. Kinetic analysis

In the presence of TiO_2 under UV-illumination, a rapid decrease of the concentration of the three

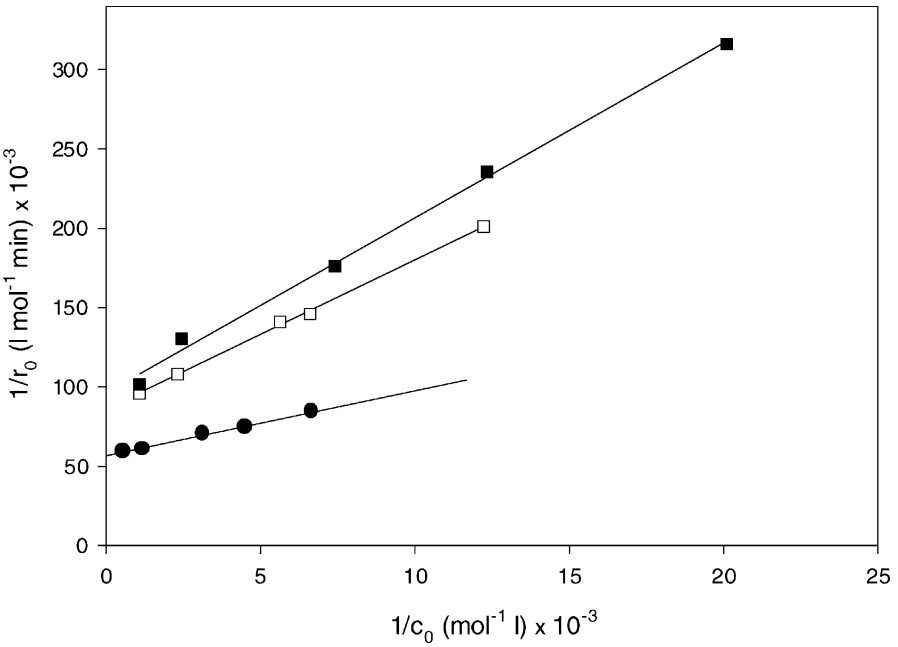

Fig. 1. Linear fitting of the $1/r_0$ vs. $1/c_0$ representations for maleic (□), fumaric (■) and oxalic acid (●). Initial pH = 3 and temperature 25 °C.

diacids is achieved. Kinetic analysis of the obtained experimental data has been performed by using the Langmuir–Hinshelwood model. The time-course of the three diacids concentration at pH = 3 were monitored and the initial degradation rates (r_0), at each one of the initial concentrations (c_0) tested were determined. In Fig. 1, the values of $1/r_0$ vs. $1/c_0$ for maleic, fumaric and oxalic acids are represented; straight lines are obtained in agreement with the Langmuir–Hinshelwood model:

$$\frac{1}{r_0} = \frac{1}{k} + \left(\frac{1}{kK}\right)\left(\frac{1}{c_0}\right) \quad (1)$$

where k is the rate constant of the photocatalytic unimolecular degradation of the adsorbed organic molecule and K the equilibrium adsorption constant. From the straight lines in Fig. 1, the kinetic parameters for the three diacids have been calculated and summarised in Table 1. As can be seen, the photodegradation rate constant decreases in the order: oxalic acid > maleic acid ≅ fumaric acid.

In spite of the experimental behaviour showed in Fig. 1, it must be considered that the fulfilment of Eq. (1) does not constitute a definite proof that an adsorption step occurs prior to chemical reaction, as predicted by the Langmuir–Hinshelwood kinetic model. In fact, it is known that experimental data for homogeneous reactions can also give $1/r_0$ vs. $1/c_0$ linear fittings [16]. Furthermore, the Langmuir–Hinshelwood model assumes adsorption consistent with Langmuir isotherm. In order to ascertain if the inherent hypothesis of such model are accomplished, some dark adsorption experiments were performed.

Table 1
Values of the rate (k) and equilibrium adsorption (K) constants for maleic, fumaric and oxalic acids, and correlation coefficients of the linear fittings of the experimental data according to the Langmuir–Hinshelwood kinetic model (initial pH = 3 and temperature = 25 °C)

Parameter	Maleic acid	Fumaric acid	Oxalic acid
k (10^{-5} mol l^{-1} min^{-1})	1.16 ± 0.04	1.05 ± 0.09	1.76 ± 0.04
K (10^3 l mol^{-1})	9.1 ± 0.3	8.7 ± 0.6	14 ± 1
Correlation coefficient	0.999	0.996	0.996

Table 2
Number of moles of diacid adsorbed onto the TiO_2 surface (n_i^s) and equilibrium concentrations of maleic, fumaric and oxalic acids in the aqueous phase ($c_{i,eq}$) in the dark (initial pH = 3 and temperature = 25 °C)

Maleic acid		Fumaric acid		Oxalic acid	
$c_{i,eq}$ (μmol l^{-1})	n_i^s (μmol)	$c_{i,eq}$ (μmol l^{-1})	n_i^s (μmol)	$c_{i,eq}$ (μmol l^{-1})	n_i^s (μmol)
930	43	918	52	1793	117
432	39	410	46	867	78
178	33	135	33	405	54
46	21	82	28	151	49

3.2. Adsorption studies

According to the Langmuir isotherm, the covering fraction (θ) can be expressed as:

$$\theta = \frac{K' c_{i,eq}}{1 + K' c_{i,eq}} \quad (2)$$

where K' is the dark equilibrium adsorption constant and $c_{i,eq}$ the concentration of the organic in such equilibrium. On the other hand, expressing θ as the ratio between the moles of organic molecules adsorbed (n_i^s) and the moles of organic adsorbed under saturation ($(n_i^s)_{sat}$),

$$\theta = \frac{n_i^s}{(n_i^s)_{sat}} = \frac{n_i^s/w}{(n_i^s/w)_{sat}} \quad (3)$$

where w is the mass of catalyst. Introducing (3) into Eq. (2) and rearranging, the following linearised form of the Langmuir isotherm is obtained:

$$\frac{c_{i,eq}}{n_i^s/w} = a c_{i,eq} + b \quad (4)$$

where $a/b = K$ and $1/a = (n_i^s/w)_{sat}$. In Table 2, the n_i^s values and the equilibrium concentrations of maleic, fumaric and oxalic acids in the aqueous phase ($c_{i,eq}$) are summarised. Fig. 2 shows the representation of $c_{i,eq}/(n_i^s/w)$ as a function of $c_{i,eq}$ for each one of the studied compounds.

As can be seen, good linear fittings are obtained for maleic and fumaric acids in the whole range of concentrations tested, while for oxalic acid, the linear behaviour is solely achieved for concentrations up to 0.4×10^{-3} mol l^{-1}. From these straight lines, the dark equilibrium adsorption constants, K', and the $(n_i^s)_{sat}$ values ($w = 0.600$ g) for the respective diacids have been calculated (see Table 3).

From these results, it must be deduced that adsorption isotherms of maleic and fumaric acids are consistent with Langmuir model, whereas such adsorption model does not successfully apply in the case of oxalic acid adsorption. In fact, experimental isotherm of oxalic acid does not show an adsorption limiting value. As must be predictable from that, oxalic acid adsorption is better adapted to a Freundlich isotherm. A good linear fitting of adsorption experimental values for oxalic acid to the Freundlich model has been obtained (correlation coefficient 0.998). This result is interpreted as non-contemptible heterogeneity of adsorption sites at high enough oxalic acid concentrations. Taking into account this limitation about the applicability of Langmuir isotherm for oxalic acid adsorption, numerical values resulting from Langmuir–Hinshelwood model cannot be considered of full validity for the whole range of concentrations studied. Thus, the correlation between adsorption (see Table 3) and kinetic (see Table 1) studies discussed below is only referred to maleic and fumaric acids.

The values of K' (see Table 3) are greater than the corresponding K values obtained from the Langmuir–Hinshelwood model application to the kinetic experimental data (see Table 1). This could be an indication

Table 3
Dark adsorption equilibrium constants (K'), number of moles of diacid adsorbed at saturation ($(n_i^s)_{sat}$) for the three diacids, and correlation coefficients of the corresponding linear fittings according to equation [4] (initial pH = 3 and temperature = 25 °C)

Parameter	Maleic acid	Fumaric acid	Oxalic acid
K' (10^4 l mol^{-1})	1.7 ± 0.3	1.2 ± 0.2	1.8 ± 0.3
$(n_i^s)_{sat}$ (μmol)	46	56	59
Correlation coefficient	0.999	0.999	0.999

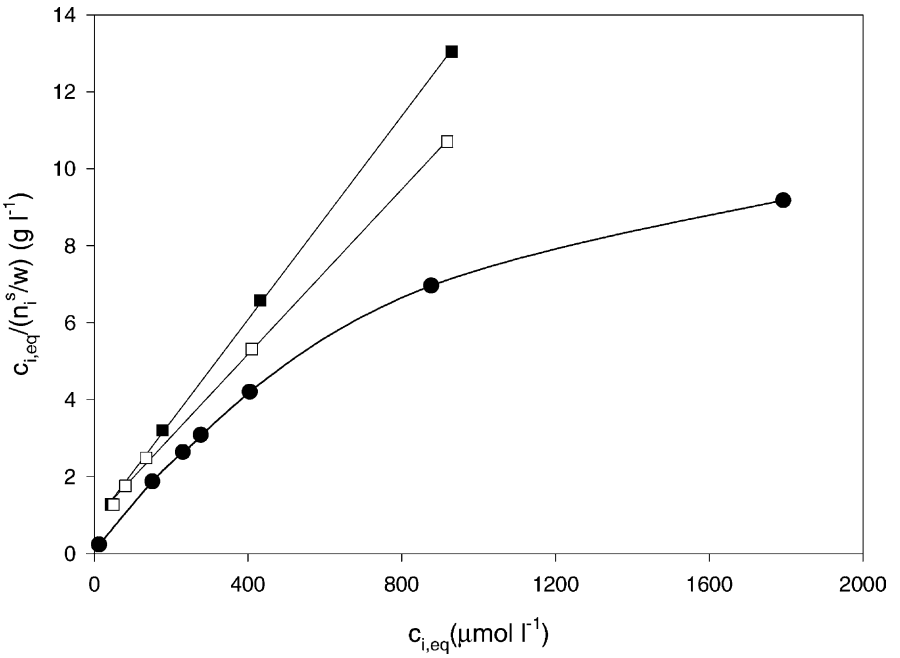

Fig. 2. Representations of $c_{i,eq}/(n_i^s/w)$ vs. $c_{i,eq}$, according to the Langmuir isotherm (Eq. (4)), for maleic (■), fumaric (□) and oxalic acid (●), at dark TiO_2 suspensions at initial pH = 3.

that a certain photodesorption occurs when the suspension is under UV-illumination [17,18]. In fact, considering a first-order reaction of the adsorbed organic diacid onto the catalyst, and assuming equal fractions of adsorbed diacid under illumination and in the dark, then the initial rate of photodegradation can be expressed as:

$$r_0 = k\theta = \frac{kn_i^s}{(n_i^s)_{sat}} \quad (5)$$

where r_0 is the initial rate of the diacid photocatalytic degradation when equilibrium dark adsorption of n_i^s moles has been attained. In Fig. 3, the r_0 values of maleic and fumaric acid photocatalytic degradation are represented as a function of the fraction of adsorbed diacid at equilibrium at different initial diacid concentration. As it is observed, the slope of the obtained straight line that corresponds to k in Eq. (5), is around 1×10^{-5} mol l^{-1} min^{-1}. This k value matches the rate constants calculated from the Langmuir–Hinshelwood kinetic model application (see Table 1). However, the straight lines are shifted about 0.2 units to the right of the origin; this implies that for a determined rate value of diacid photodegradation, a lower degree of adsorption than the predicted from adsorption equilibrium values prior to illumination occurs, and therefore a certain photodesorption can be assumed when semiconductor particles are illuminated.

3.3. Effect of pH

The photocatalytic degradation of the three diacids at some different initial pH values between 3 and 9 has been studied. In Fig. 4, the initial rate of diacid photodegradation (r_0) as function of initial pH is depicted. In the case of oxalic acid, a gradual decrease of r_0 with increasing the initial pH occurs, while for maleic and fumaric acids a different behaviour is noticed: a decrease of r_0 with increasing pH at acid media, and the opposite trend at higher pH media.

On the other hand, from dark adsorption data (see Fig. 5) a decrease of the mass of organic adsorbed with increasing the initial pH for the three diacids is observed. This trend is noticed to be more pronounced at pH values lower than the point of zero charge (pzc) of TiO_2 (6.25 [19]) and agrees with the pH effects

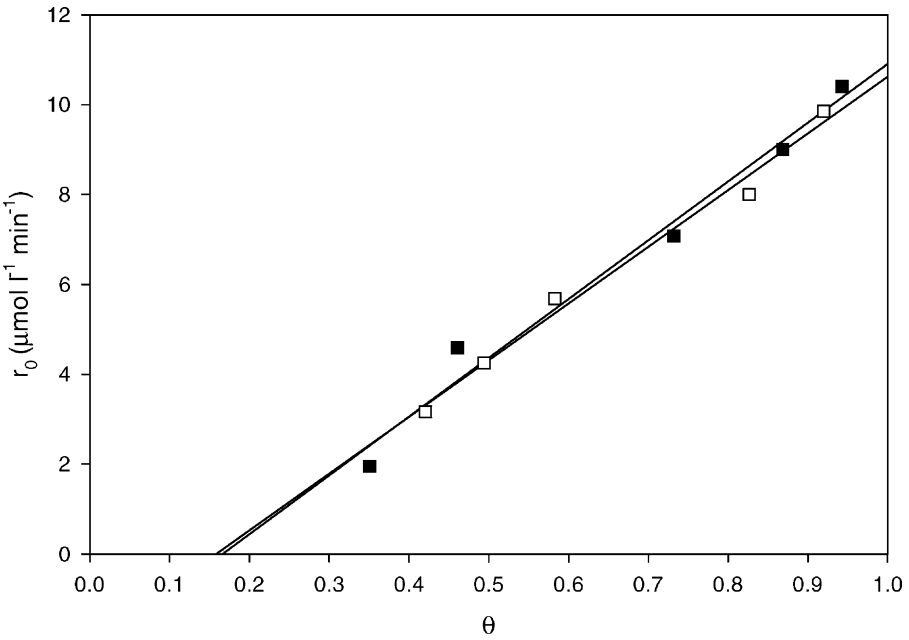

Fig. 3. Initial rates of photocatalytic degradation as a function of θ for maleic (■) and fumaric (□) acids, from TiO_2 suspensions at 1×10^{-3} mol l^{-1} of diacid concentration at 25 °C.

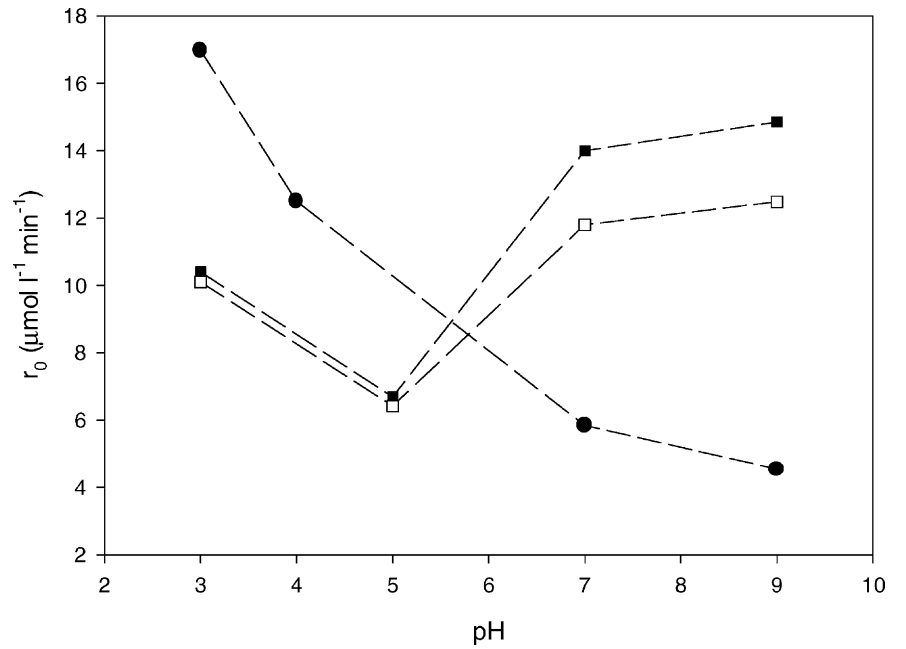

Fig. 4. Initial rates of photocatalytic degradation as a function of initial pH of maleic (■), fumaric (□) and oxalic acids (●), for TiO_2 suspensions of 1×10^{-3} mol l^{-1} at 25 °C.

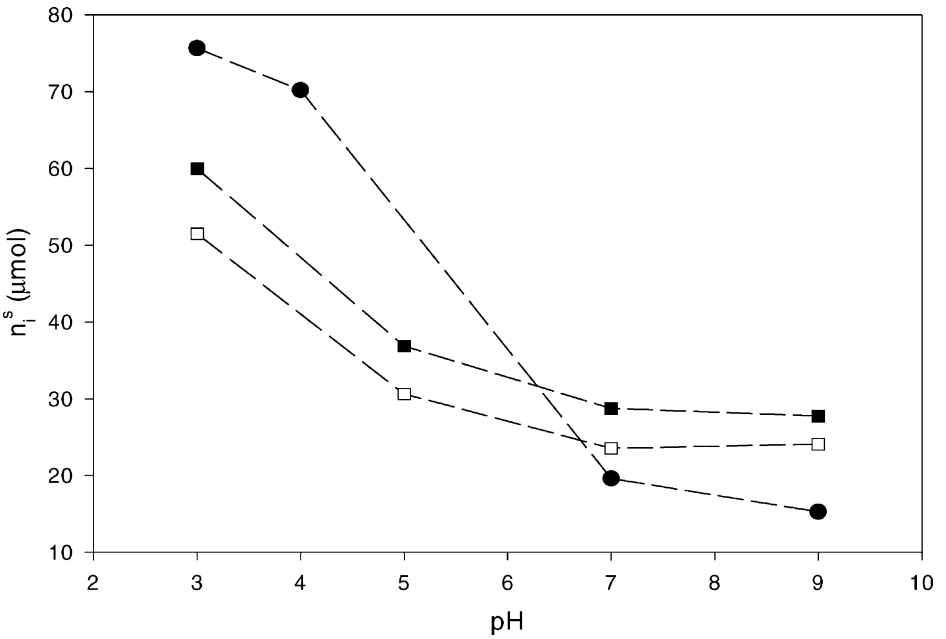

Fig. 5. Moles of maleic (■), fumaric (□) and oxalic acids (●) adsorbed onto TiO_2 (0.6 g) in the dark at different initial pH.

upon acid–base equilibrium on the catalyst surface and species in solution. Such equilibrium leads to the lacking of positive surface charges on the catalyst and the increasing of negatively charged species concentration in solution with increasing pH, enlarging the electrostatic repulsion between organic substrates and TiO_2 surface.

From these observations, it seems clear that in order to degrade oxalic acid a previous adsorption step must occur. Maleic and fumaric acids, behave like oxalic at pH lower than the semiconductor pzc; however, at higher initial pH, a significant increase of the photodegradation rate with increasing pH occurs (see Fig. 4). Considering that such behaviour is observed in spite of the low degree of adsorption observed at these pH media (see Fig. 5), it can be suggested that the degradation of these diacids takes place mainly in homogeneous phase by reacting with photogenerated $OH^\bullet$ radicals. Thus, $OH^\bullet$ radicals, which are more favourably produced at alkaline pH, once formed at the surface of the semiconductor, diffuse to the bulk of the solution where they react with the diacid molecules [16,20]. Thereby, it is feasible to correlate the similar increase in degradation rate for both isomers with the pH effect on $OH^\bullet$ radical concentration. Furthermore, at pH > pzc (TiO_2), when isomerisation is not observed (see below), degradation rate becomes significantly greater for maleic than for fumaric acid. This agrees with a degradation pathway controlled by an homogenous oxidation reaction, since maleic acid oxidation should be easier than fumaric oxidation, in accordance with the instability of the *cis* conformation due the electrostatic repulsion between the carboxylate groups negatively charged at such pH conditions. On the other hand, the pH effect on r_0 is not probably due to a change in the rate determining step, since degradation rate depends on substrate concentration for the whole rang of pH tested.

The supposed change with pH in the main pathway of maleic acid degradation has been confirmed by experiments performed in presence of methanol; this compound shows a very low degree of adsorption and efficiently reacts with $OH^\bullet$ radicals in homogeneous phase [21–23]. Then, for example, in aqueous TiO_2 suspensions of maleic acid (1×10^{-3} mol l^{-1}), the observed initial rate of maleic degradation at initial pH = 9 is significantly decreased in presence of methanol (0.1 mol l^{-1}): 1.4×10^{-5} mol l^{-1} min^{-1} vs.

0.7×10^{-5} mol l^{-1} min^{-1}, while at initial pH = 3 the presence of methanol does not affect the maleic acid degradation efficiency, resulting the observed rate value of 1×10^{-5} mol l^{-1} min^{-1} either in absence or in presence of methanol. This confirms that in alkaline media the main route of maleic acid (and fumaric acid) oxidation in homogeneous phase is the attack by $OH^{\bullet}$, whose availability is affected by the presence of methanol; while in acid media the presence of methanol does not affect the rate of maleic acid degradation because the process occurs in the adsorbed phase.

3.4. Intermediates and mechanism of the reaction

The three diacids are photocatalytically degraded to CO_2. In Fig. 6, both the TOC in solution and the organic carbon corresponding to fumaric and oxalic acids, at initial pH values 3 and 9, are represented (the data for maleic acid is not depicted because it shows a similar behaviour than the observed for fumaric acid). From this plot, fumaric acid (and also maleic acid) removal at acid pH occurs much earlier than total mineralisation. It means that a build-up of intermediates is produced; at alkaline pH the time-course of both diacid elimination and TOC become closer. In the case of oxalic acid at pH = 3, the time-course of diacid elimination matches TOC disappearance at shortest times of illumination and they keep close afterwards. At pH = 9 both, TOC elimination and oxalic acid is noticeable reduced, showing significant differences between both time-courses.

From HPLC analysis, some intermediates of the photocatalytic process have been identified. For both maleic and fumaric acids at pH = 3, the appearance of an intermediate at short irradiation times has been detected. This intermediate has been identified as fumaric acid during maleic acid photodegradation, and maleic acid during fumaric acid photodegradation. Therefore, a *cis–trans* isomerisation of both organic diacids takes place. The *cis–trans* isomerisation of olefins over TiO_2 and CdS photocatalysts has been well documented, and it is supposed to be mediated by the interaction between the adsorbed olefin and the photogenerated holes at semiconductor surface [24–26]. It must be pointed out that no evidences of *cis–trans* isomerisation are observed at pH = 9. This is consistent with the non-significant adsorption occurring at alkaline pH values.

According to the observed isomerisation process, it is not surprising that the same degradation k values (see Table 1) and the same intermediate products (i.e. malic, acrylic, acetic, oxalic and formic acids) have been detected during photocatalytic degradation of maleic and fumaric acids at pH < pzc (TiO_2). The acrylic acid yield, that can be calculated from its time-course concentration profile, indicates that its formation is the main route of both isomers disappearance. Thereby, the fumaric and maleic acid degradation process can be proposed to take place mainly trough a photo-Kolbe reaction. Furthermore, this assumption agrees with their preadsorption as a requirement for their degradation at pH < pzc (TiO_2).

It has been previously proposed that the photocatalytic degradation of fumaric and maleic acids takes place trough two different pathways following these sequences [4]:

1. maleic/fumaric → acrylic → acetic → formic → CO_2,
2. maleic/fumaric → tartaric → tartronic → glycolic → glyoxylic → oxalic → formic → CO_2.

During maleic or fumaric acid photocatalytic degradation, we have not detected intermediates such as tartaric, glycolic nor glyoxylic acids in our system, but acetic, oxalic and formic acids as previously mentioned. The route that leads to oxalic formation seems to be less important, or otherwise, the intermediates implied have to be easily degraded since oxalic acid has been detected at very low concentration. Finally, malic acid formation indicates that H–OH addition to the double bond can occur as a first step of maleic and fumaric acid elimination. However, taking into account the low concentration of malic acid found and, as previously mentioned, the fact that acrylic acid formation nearly explains the maleic and fumaric acid disappearance, it can be assumed that malic generation pathway represents a poor contribution to these isomers degradation. Moreover, feasible intermediates of malic acid degradation process as lactic acid, malonic acid and acetaldehyde have not been detected. In Scheme 1, the reaction sequence for maleic and fumaric acid degradation at pH < pzc (TiO_2) is detailed.

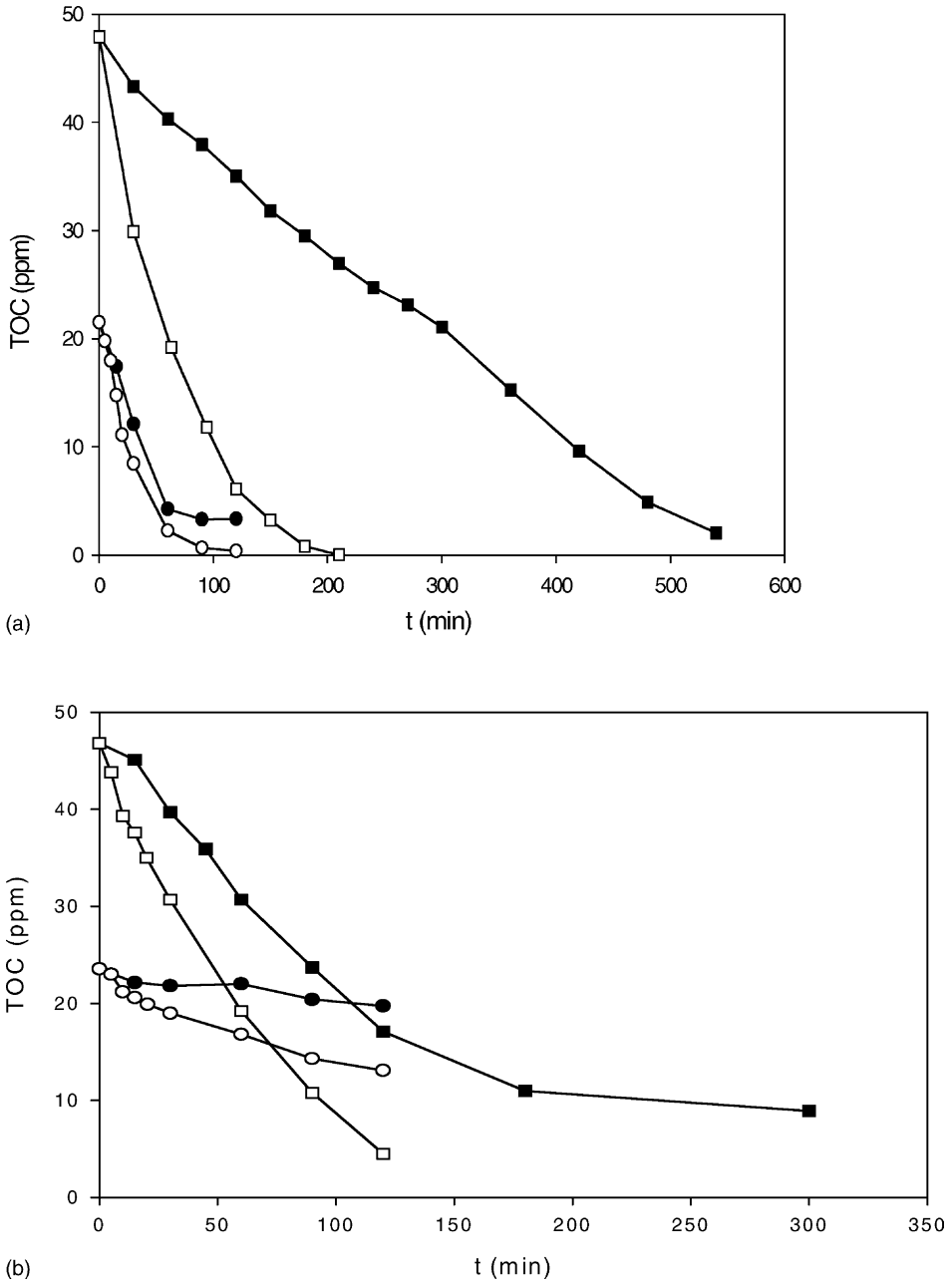

Fig. 6. Time-course of the TOC in solution (dark symbols) and organic carbon corresponding to diacid (white symbols) for fumaric (■ and □) and oxalic (● and ○) acids at initial pH of 3 (a) and pH of 9 (b) in presence of TiO_2 under UV-illumination.

The same intermediates have been detected during fumaric and maleic acid degradation at pH > pzc (TiO_2). It must be reminded that at initial pH = 9, TOC removal is closer to maleic or fumaric acid degradation than at pH = 3 (see Fig. 6). Detected intermediates during the first hour appear at much lower concentration than for degradation performed at pH = 3. These intermediates are malic, acetic and formic

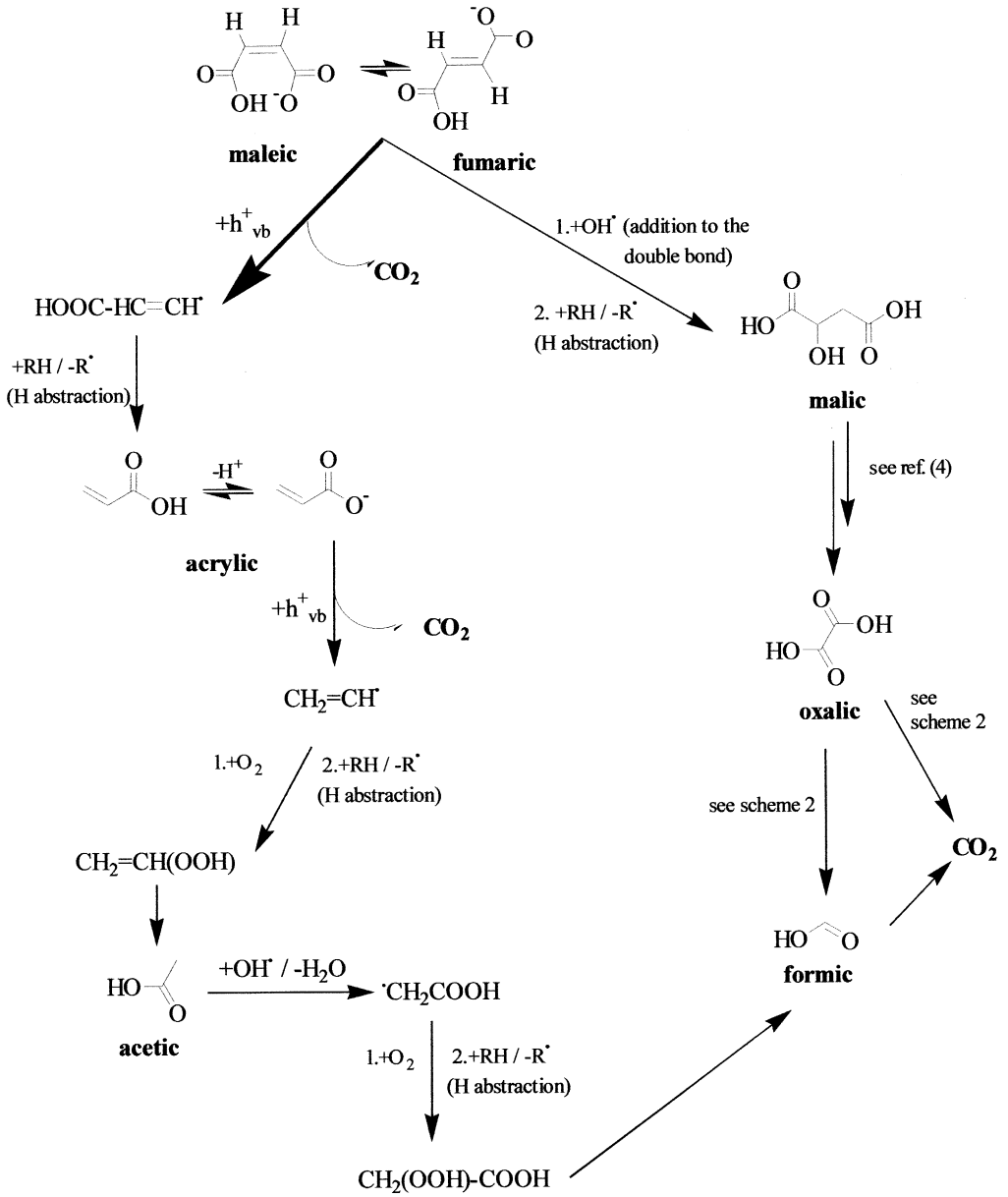

Scheme 1. Reaction scheme for maleic and fumaric acid degradation at pH < pzc (TiO_2). R–H corresponds to any organic with suitable hydrogen to abstract.

acids. Acrylic acid is not detected during degradation at initial pH = 9, accordingly with an homogeneous oxidation (with photogenerated $OH^{\bullet}$ radicals) instead of an heterogeneous oxidation as the rate determining step. At this higher pH conditions, the photo-Kolbe process is not expected to be favoured due to different facts: the lower oxidation power of valence band holes with increasing pH, and the existing large distance between catalyst surface and non-adsorbed organic molecule both negatively charged. Following with the

analysis of the TOC time-course, it has been observed that when fumaric and maleic acids are totally eliminated from aqueous solution, there is about a 20% of remaining TOC with a slow elimination rate. At that point, oxalic acid is the only intermediate detected. Moreover, oxalic acid appears at a concentration value that matches with the remaining TOC. Then it can be assumed that, at pH > pzc (TiO_2), there are different feasible degradation routes for fumaric and maleic acid degradation. Each intermediates different from oxalic acid are easily eliminated, and such degradation is easier than at pH = 3 for malic and acetic acids. Thus oxalic acid constitutes the remaining TOC.

In the case of the photocatalytic oxidation of oxalic acid only formic acid has been detected. From the results obtained in the present work, it seems clear that the photocatalytic degradation of oxalic acid mainly occurs in heterogeneous phase. The photo-Kolbe reaction is the first step of the mechanism (Scheme 2).

The assumption of photo-Kolbe process as the main route of oxalic disappearance is in agreement with the preadsorption as a requirement for oxalic acid degradation. Thereby, from results at pH = 7 and 9 it can be assumed that $OH^{\bullet}$ radicals are not active enough for oxalic acid oxidation. It is suggested that steps 2 and 4 can take place either in homogeneous or heterogeneous phase. At pH = 9, for which practically no adsorption occurs, a direct photolytic degradation process can be assumed (see discussion of blank experiments) as the main route of oxalic acid concentration reduction during the irradiation period.

1. $^{-}OOC-COO^{-}(ads) + h^{+}(ads) \rightarrow CO_2 + CO_2^{\bullet -}(ads)$
2. $CO_2^{\bullet -} + OH^{\bullet} \rightarrow CO_2 + OH^{-}$
3. $CO_2^{\bullet -}(ads) + h^{+}(ads) \rightarrow CO_2$
4. $CO_2^{\bullet -} + H_2O \rightarrow HCOO^{-} + OH^{\bullet}$
5. $HCOO^{-}(ads) + h^{+}(ads) \rightarrow HCO_2^{\bullet}$
6. $HCO_2^{\bullet} + OH^{\bullet} \rightarrow CO_2 + H_2O$

Scheme 2. Reaction scheme for oxalic acid photocatalytic degradation.

3.5. Multicomponent system

In order to investigate the kinetics of diacid degradation for a multicomponent system containing the three diacids, some experiments of photocatalytic

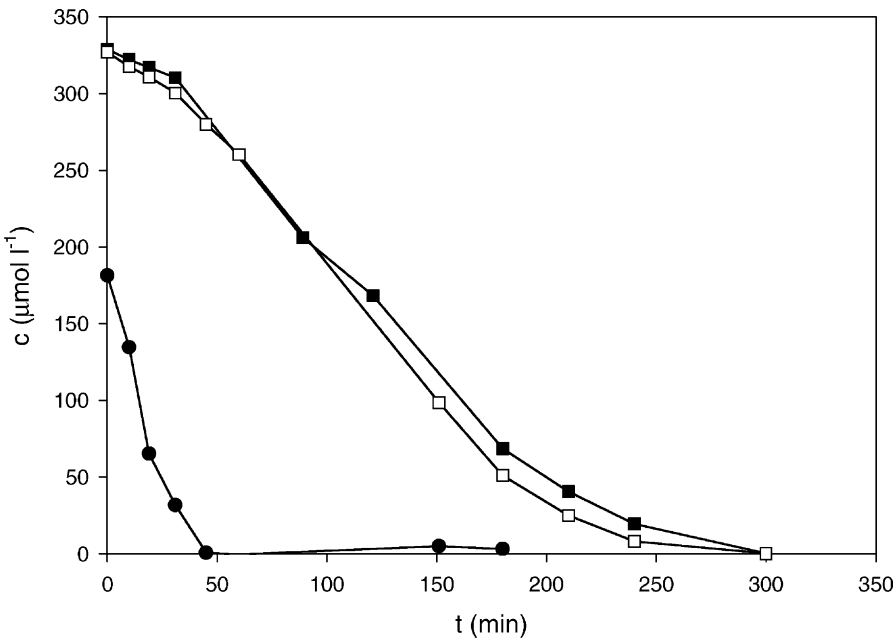

Fig. 7. Time-course of maleic (■), fumaric (□) and oxalic acids (●) in a multicomponent system at pH = 3 in presence of TiO_2 under UV-illumination.

Table 4
Experimental ($r_{0,exp}$) and theoretical ($r_{0,th}$) initial rates of photodegradation for maleic, fumaric and oxalic acids for the multicomponent system of total concentration 1×10^{-3} mol l^{-1} at initial pH = 3 and 25 °C of temperature

Parameter	Maleic acid	Fumaric acid	Oxalic acid
$r_{0,exp}$ (μmol l^{-1})	0.6	0.8	4.7
$r_{0,th}$ (μmol l^{-1})	3.6	3.4	5.6
$r_{0,th}/r_{0,exp}$	6.0	4.0	1.2

degradation in aqueous TiO_2 suspensions at pH = 3 were carried out. Fig. 7 shows the time-course of maleic, fumaric and oxalic acid concentrations (0.33×10^{-3} mol l^{-1}) for an irradiated 1×10^{-3} mol l^{-1} total organic solution at an initial pH = 3 in presence of TiO_2.

From dark equilibrium adsorption data (point at $t = 0$ in Fig. 7, it can be seen that fumaric and maleic acid molecules practically do not adsorb onto the TiO_2 surface, being the adsorption sites saturated by oxalic acid molecules. Table 4 summarises the initial rates calculated from experimental data depicted in Fig. 7 and the theoretical values obtained from the application of the Langmuir–Hinshelwood kinetic model to a multicomponent system:

$$r_{0,i} = \frac{k_i K_i c_i}{1 + \sum_j K_j c_j} \quad (6)$$

using the k and K values of the three diacids corresponding to the unicomponent systems (see Table 1). Within the experimental error, similar theoretical and experimental values are only observed for oxalic acid, while for maleic and fumaric acids experimental values much lower than the theoretical ones are noticed.

As it is observed from Fig. 7, the slope of the time-course of fumaric and maleic concentrations significantly increases after a certain time period, when enough oxalic acid molecules have been degraded and then corresponding adsorption sites have been released to accommodate fumaric and maleic acid molecules, promoting degradation at pH = 3. In fact, for a bicomponent fumaric–maleic acid system (c_0(maleic) = c_0(fumaric) = 0.5 mM) in the absence of oxalic acid, photocatalytic degradation of both isomers follows the Langmuir–Hinshelwood kinetic model, since experimental initial photodegradation rates at such system are predictable by using Eq. (6) with k and K values shown in Table 1.

4. Conclusions

The photocatalytic degradation of maleic, fumaric and oxalic acids is highly dependent on the pH. At pH lower than the pzc of TiO_2, the photodegradation with a previous adsorption step occurs and the Langmuir–Hinshelwood kinetic model within a certain concentration range can be assumed; the rate constant of photodegradation decreases in the order: oxalic acid > maleic acid ≅ fumaric acid acid. An initial photo-Kolbe step is suggested. For oxalic acid photocatalytic degradation, direct mineralisation mainly occurs, and formic acid at very low concentration is detected as the only intermediate product. For maleic and fumaric acids, a *cis–trans* isomerisation induced by interaction between adsorbed diacid and semiconductor surface occurs. Photo-Kolbe and $OH^{\bullet}$ attack on diacid molecules also takes place, generating the build-up of different intermediate products (acrylic, malic, acetic, oxalic and formic acids). At pH higher than the pzc of TiO_2, adsorption of the three diacids is of low significance. In spite of this, good yields of photocatalytic degradation of fumaric and maleic acids mediated by $OH^{\bullet}$ radicals in homogeneous phase are obtained, and *cis–trans* isomerisation it is not observed. At such conditions, oxalic acid is the main intermediate and its formation implies a low degradation rate of the remaining TOC. This is consistent with the observed pH effect on oxalic photodegradation rate, that noticeably decreases with increasing pH.

For multicomponent systems at pH lower than the pzc of the TiO_2, oxalic acid molecules preferentially occupy the adsorption sites of the TiO_2 surface being more easily degraded than maleic and fumaric acids. For bicomponent system containing maleic and fumaric acids at pH < pzc, the photocatalytic degradation follows the Langmuir–Hinshelwood model kinetics.

Acknowledgements

The authors wish to thank to CICYT (project: AMB99-1212-C03-01) for financial support. They

also thank the CYTED network VIII-G for supporting the publication of this work.

References

[1] J.-M. Herrmann, C. Guillard, J. Disdier, C. Lehaut, S. Malato, J. Blanco, Appl. Catal. B 35 (2002) 281.
[2] M.R. Hoffmann, S.T. Martin, W. Chei, D.W. Bahnemann, Chem. Rev. 95 (1995) 69.
[3] A. Mills, S. Le Haunte, J. Photochem. Photobiol. A 108 (1997) 1.
[4] J.M. Herrmann, H. Tahiri, C. Guillard, P. Pichat, Catal. Today 54 (1) (1999) 131.
[5] C. Galindo, P. Jacques, A. Kalt, J. Photochem. Photobiol. A 130 (2000) 35.
[6] A. Assabane, Y. Ait Ichou, H. Tahiri, C. Guillard, J.-M. Herrmann, Appl. Catal. B 24 (2000) 71.
[7] C. Guillard, J. Photochem. Photobiol. A 135 (2000) 65.
[8] E. Brillas, E. Mur, R. Sauleda, L. Sánchez, J. Peral, X. Domènech, J. Casado, Appl. Catal. B 16 (1998) 31.
[9] R. Sauleda, E. Brillas, Appl. Catal. B 29 (2001) 135.
[10] A. Balcioglu, N. Getoff, M. Bekbölet, J. Photochem. Photobiol. A 135 (2000) 229.
[11] J.R. Harbour, M.L. Hair, J. Phys. Chem. 83 (1979) 652.
[12] J.M. Herrmann, M.N. Mozzanega, P. Pichat, J. Photochem. 22 (1983) 333.
[13] J. Domènech, J.M. Costa, Photochem. Photobiol. 44 (1986) 675.
[14] J. Domènech, J. Peral, J. Chem. Res. (1987) 360.
[15] X. Domènech, J.A. Ayllón, J. Peral, Environ. Sci. Pollut. Res. 8 (2001) 285.
[16] C.S. Turchi, D.F. Ollis, J. Catal. 122 (1990) 178.
[17] M.A. Fox, M.T. Dulay, Chem. Rev. 93 (1993) 341.
[18] A. Mills, S. Le Haunte, J. Photochem. Photobiol. A 108 (1997) 1.
[19] M.R. Hoffmann, S.T. Martin, W. Chei, D.W. Bahnemann, Chem. Rev. 95 (1995) 69.
[20] C. Jaussaud, O. Paissé, R. Fauré, J. Photochem. Photobiol. A 130 (2000) 157.
[21] J. Cunningham, P. Sédlak, J. Photochem. Photobiol. A 77 (1994) 255.
[22] Y. Mao, C. Schöneich, K.-D. Asmus, J. Phys. Chem. 95 (24) (1991) 10080.
[23] C. Galindo, P. Jacques, A. Kalt, J. Photochem. Photobiol. A 130 (2000) 35.
[24] M.A. Fox, C.C. Chen, J. Am. Chem. Soc. 103 (1981) 6757.
[25] S. Yanagida, K. Mizumoto, C. Pac, J. Am. Chem. Soc. 108 (1996) 647.
[26] J. Araña, O. González Díaz, M. Miranda Saracho, J.M. Doña Rodríguez, J.A. Herrera Melián, J. Pérez peña, Appl. Catal. B 36 (2002) 113.